use. Seven micrometers of coronal frozen sections were cut on a cryostat JUNG CM 3000 (Lica), mounted onto silanized slides (DAKO), air-dried, and stored at −80 °C until were used for immunohistochemistry.

2.4. Western blotting

Rats were anesthetized with diethylether 6 h after spinal cord impaction and their spinal cord from the top and bottom 1.5 cm (100 mg) of the lesion were dissected, homogenized in 10 times of the sample buffer (62.5 mM Tris, pH 6.8, 2% SDS, 10% glycerol, 5% 2-mercaptethanol, and 0.01% bromophenol blue), lysed, and denatured. Five mircoliters of each sample was loaded on to an 8% SDS–polyacrylamide gel. Proteins were transferred to a nitrocellulose membrane. The membrane was probed with mouse monoclonal antibody to COX-2 (dilution: 1:100; Transduction) and proteins were detected using a chemiluminescent detection system (Amersham Bioscience).

2.5. Immunohistochemistry

Spinal cord sections were incubated in blocking solution (10% normal donkey serum with 0.4% Triton X-100 in PBS) for 30 min, COX-2 antibody for 48 h at 4 °C, and Cy3-conjugated donkey anti-rabbit IgG for 1 h. For double staining, the sections were incubated with the appropriate combination antibodies against COX-2, iNOS, or cell-specific monoclonal antibodies. After washing with PBS, they were stained with a combination of FITC-labeled anti-rabbit IgG or Cy3-labeled anti-mouse IgG for 1 h. They were rinsed in PBS, mounted with Fluoroguard (Bio Rad),

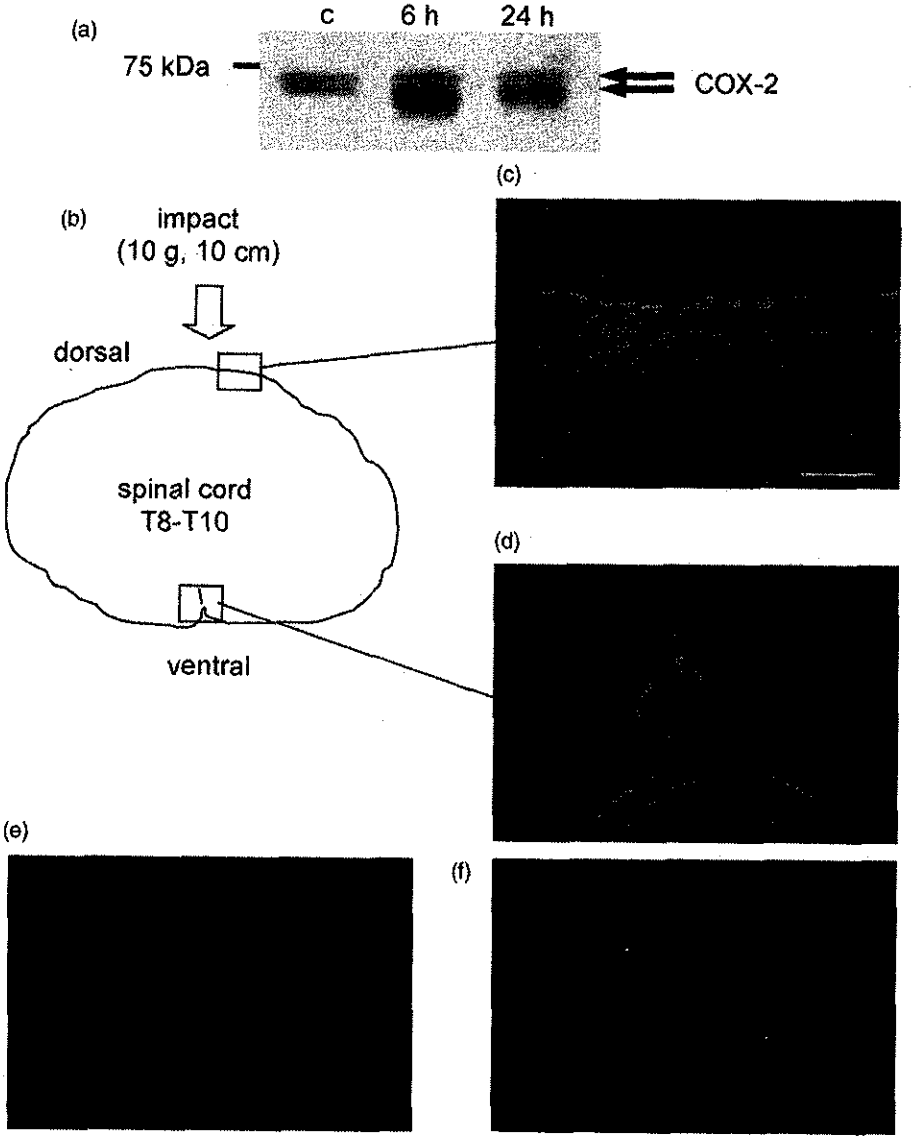

Fig. 2. (a) Western blot analysis of protein extracts obtained from spinal cord of rat 6 h and 24 h after traumatic spinal cord injury (SCI) and control rat. (b) A sketch of rat spinal cord (T8–T10) where each photograph of immunofluorescent staining specimen was obtained. Immunofluorescent staining for COX-2 in rat spinal cord around the perivascular zone (c and e) and pia matter (d and f); 6 h after traumatic SCI (c and d) or normal control (e and f). COX-2 positive cells were visualized with FITC-conjugated donkey antibody against rabbit IgG as a secondary antibody. Scale bar = 50 μm.

and examined under a fluorescent microscope with a camera attachment (Olympus).

2.6. Antibodies for immunohistochemistry

Rabbit anti-COX-2 polyclonal antibody was purchased from Cayman and used at 1:200 dilution. Mouse anti-COX-2 monoclonal antibody was purchased from Transduction and used at 1:100 dilution. Rabbit anti-iNOS polyclonal antibody was prepared using GST–iNOS (N-terminal) fusion protein as reported previously (Fan et al., 1995) and used at 1:250 dilution. Cell-specific monoclonal antibodies were purchased and used as described below: ED1, specific for monocyte, macrophage, and dendritic cells (BMA Biomedical) at 1:500; ED2, specific for macrophage (BMA Biomedical) at 1:500; OX42, specific for macrophage and microglia (BMA Biomedical) at 1:100; Cy3-conjugated glial fibrillary acidic protein (GFAP) for astrocyte (Sigma) at 1:400; MAP2, specific for neuron (Chemicon) at 1:200; and RECA-1, specific for endothelial cells (Monosan) at 1:200 Fluorescent secondary anti-mouse and rabbit antibodies (Chemicon) at 1:100 were also used.

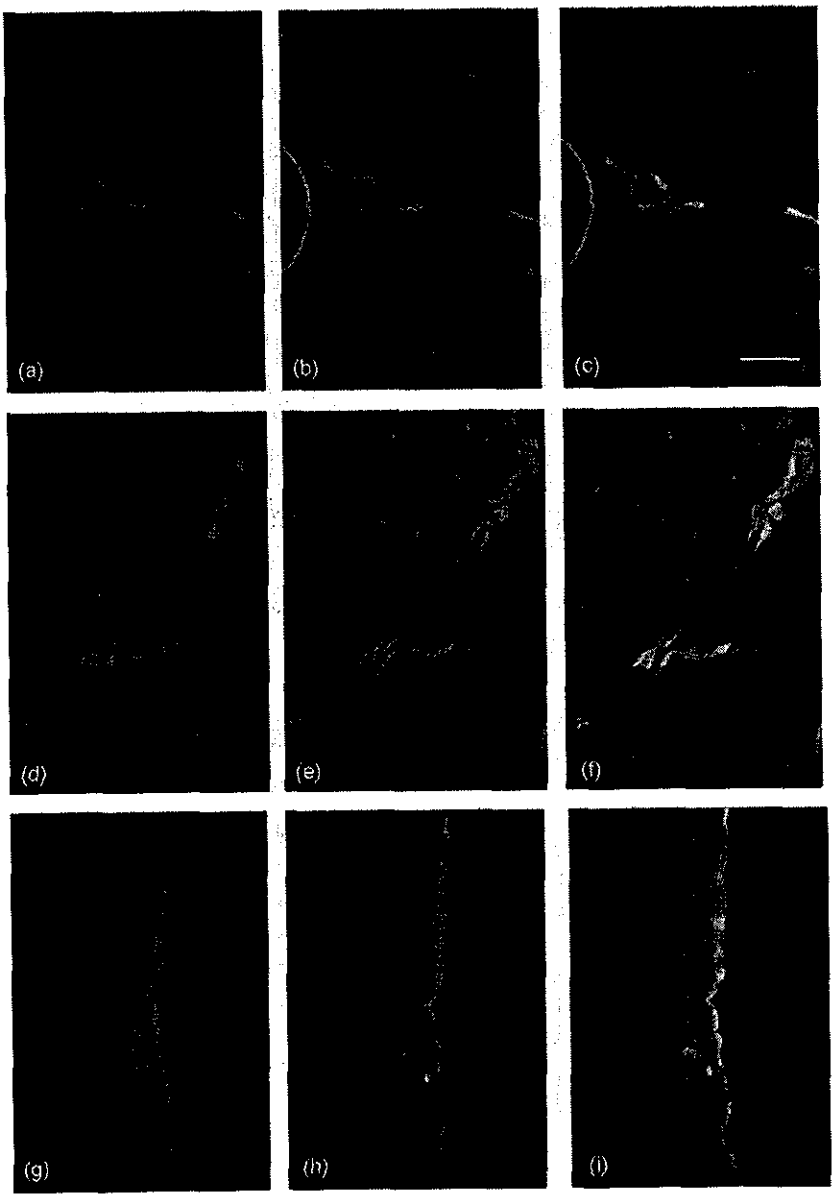

Fig. 3. Double-immunofluorescent staining of rat spinal cord, 6 h after traumatic SCI for COX-2 (green) and cell-specific markers (red). COX-2 positive cells were visualized with FITC-conjugated donkey antibody against rabbit IgG as a secondary antibody (a, d, g, j, m, p, s, and v). GFAP (n) was visualized using Cy3-conjugated mouse monoclonal antibody, and RECA-1 (b, e, and h), MAP2 (k), ED1 (q), ED2 (t), and OX-42 (w) immunoreactivities were visualized with Cy3-conjugated donkey antibody against mouse IgG as a secondary antibody. COX-2 positive cells were observed around the perivascular zone (b), the blood vessel (e), and pia matter (h), but did not coincide with MAP2 (k), GFAP (n), ED1 (q), ED2 (t), and OX42 (w) positive cells. COX-2 positive cells were shown in yellow by superimposing the two color images (c, f, and i). Scale bar = 50 μm. (For interpretation of the references to colour in this figure legend, the reader is referred to the web version of the article).

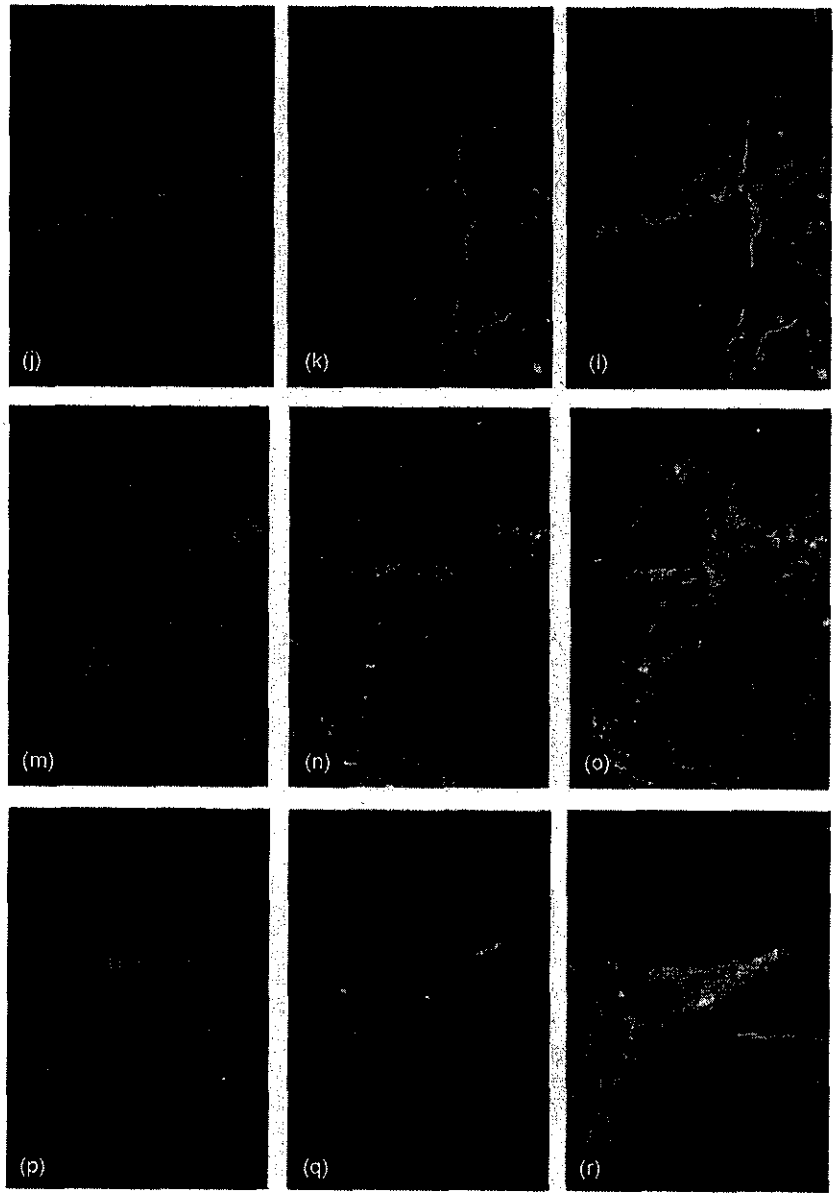

Fig. 3. (*Continued*).

3. Results

Hematoxylin–Eosin staining was performed to observe the spread of damage following weight drop impact on the rat spinal cord. Damage caused by traumatic SCI spread from the dorsal white matter to central gray matter 6 h after the injury and even the ventral gray matter began to become cavernous 3 days after the injury (data not shown, Satake et al., 2000a). First, we confirmed the time-course of COX-2 induction in the spinal cord after the injury using semi-quantitative RT-PCR. COX-2 mRNA began to increase within 30 min, peaked at 3 h, gradually began to decline at 6 h, and returned to basal levels about 1 week after the injury (Fig. 1). Sequence analysis confirmed that the 209-bp band corresponded to the rat COX-2 cDNA fragment. Next, COX-2 protein level and localization were examined in the spinal cord after traumatic SCI. Western blotting analysis showed that COX-2 protein significantly increased 6 h and remained at a high level until 24 h after the injury compared with those in control animals (Fig. 2a). Although COX-2 protein has been previously reported to compose of 72 kDa and 74 kDa forms due to the heterogeneity of *N*-glycosylation (Otto et al., 1993; Garavito et al., 2002), only the smaller one was increased by the traumatic insults to the spinal cord. Using an immunohistochemical method, the spatial expression pattern of COX-2 protein induced in the spinal cord after traumatic SCI was investigated. Six hours after injury, COX-2 immunoreactivity was detected along the pia matters and blood vessels around the contused spinal cord (Fig. 2c and d), whereas no COX-2-positive cells were detected in any cells of the normal controls (Fig. 2e and f). Next, we performed double-immunofluorescence labeling to identify COX-2-positive cell types. COX-2-positive cells were positive for RECA-1, the marker protein of endothelial

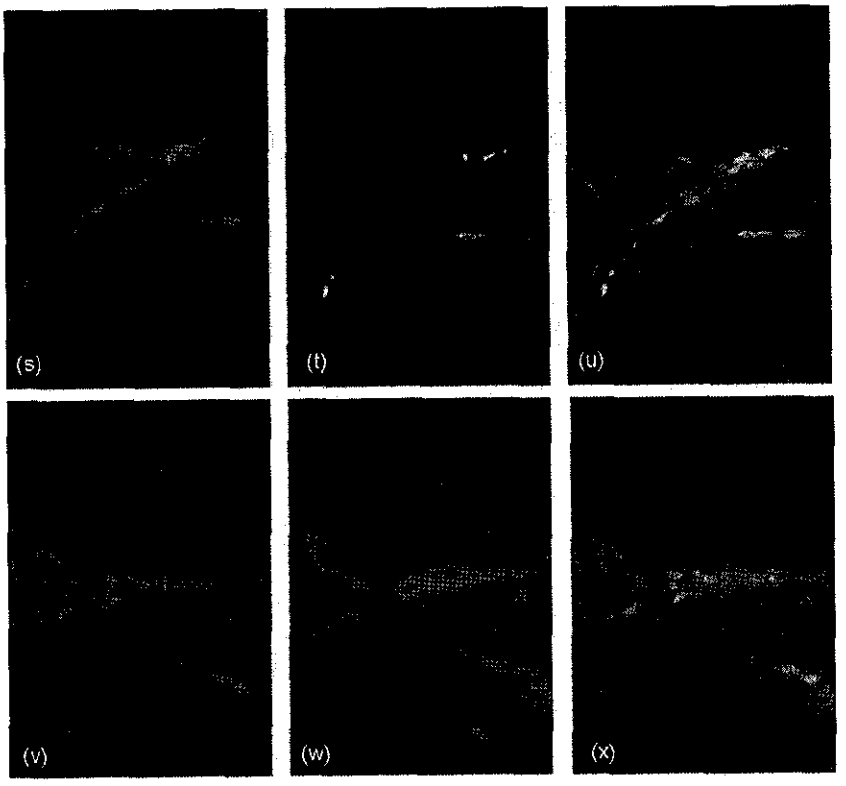

Fig. 3. (*Continued*).

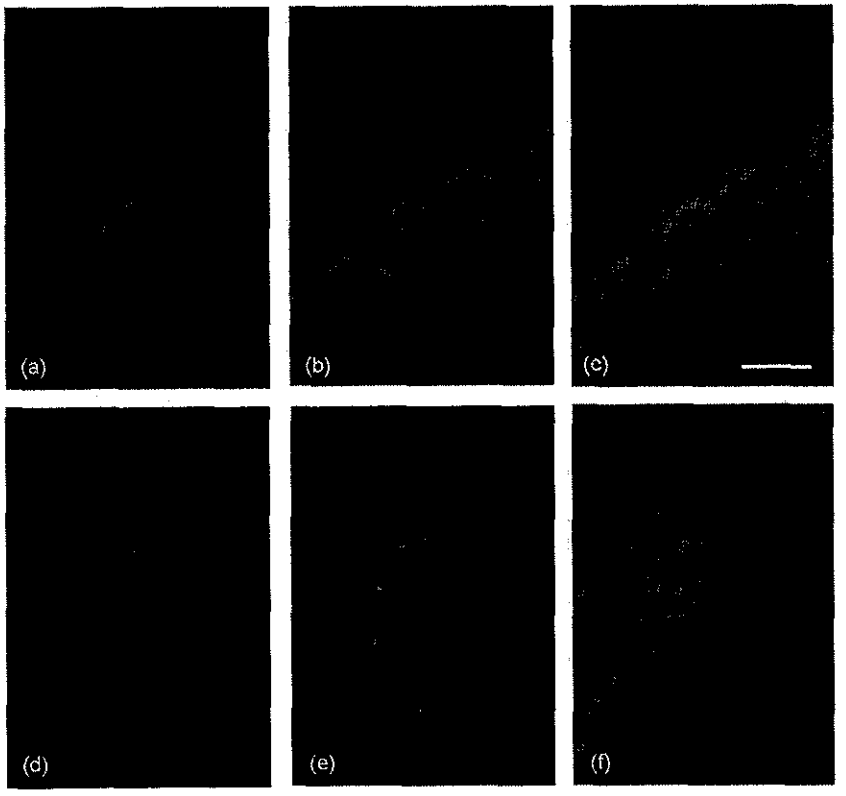

Fig. 4. Double-immunofluorescent staining of rat spinal cord injury, for COX-2 (red) and iNOS (green). COX-2 positive cells were visualized with Cy3-conjugated donkey antibody against mouse IgG as a secondary antibody (a and d). iNOS positive cells were visualized with FITC-conjugated donkey antibody against rabbit IgG as a secondary antibody (b and e). Superimposing the two-color images show that COX-2-positive cells were negative for iNOS and vice versa, and that there were some COX-2 positive cells nearby iNOS-positive cells (c and f). Scale bar = 50 μm. (*For interpretation* of the references to colour in this figure legend, the reader is referred to the web version of the article).

cells, in spinal cord 6 h after the injury (Fig. 3a–i). However, the COX-2 immunoreactivity in the spinal cord did not coincide with MAP2, GFAP, ED1, ED2, or OX42 expressed by neurons, astrocytes, monocytes, macrophages, or microglia, respectively, (Fig. 3j–x). Finally, we examined the spatial positional relation of COX-2 and iNOS after SCI. Six hours after injury, iNOS-positive cells appeared in intra-and perivascular zones, while some were scattered in the damaged area. There were some iNOS-positive cells standing nearby COX-2-positive cells (Fig. 4).

4. Discussion

We investigated the early stage temporal and spatial expression of *COX-2* gene after traumatic SCI. We found that *COX-2* gene was already induced at a half-maximal level 30 min after injury and COX-2 protein accumulation was observed in endothelial cells of blood vessels 6 h after injury. In cases of *COX-2* gene induction, Resnik reported that by using in situ hybridization COX-2 mRNA expression was detected in spinal cord neurons and around blood vessels at 2 h, 4 h, and 8 h following impaction (Resnick et al., 1998) and Tonai reported that by using Northern blotting COX-2 mRNA level was seen to increase 2 h after compression of the spinal cord (Tonai et al., 1999). In our experiment, *COX-2* gene induction after the injury was found to begin within 30 min; therefore, it seems that no new protein synthesis is required for its transcription. In addition, this immediate early expression in the spinal cord coincides well with those of iNOS (Satake et al., 2000a) and GDNF (Satake et al., 2000b). Therefore, it was postulated that the *COX-2* gene expressed in endothelial cells in addition to iNOS in macrophages and GDNF in microglia and macrophages seems to be induced by a common unidentified trigger that stimulates a pathway toward the NF-κB signaling. There are few reports of the localization of COX-2 after SCI (Resnick et al., 1998; Tonai et al., 1999), and none of them directly defined the types of cells or tissues where COX-2 protein was induced. Tonai reported that no clear expression of COX-2 was detected in any particular cell at 8 h after the injury, but instead showed that COX-2 protein was detected in polymorphonuclear leukocytes, glial cells, and vascular endothelial cells after intraparenchymal injection of 2 ng IL-1α, suggesting that induction of *COX-2* gene may be mediated by IL-1α (Tonai et al., 1999).

In this study, COX-2 protein induced after the acute injury was clarified to localize in endothelial cells using immunohistochemical double staining. However, we previously reported that iNOS-positive cells, macrophages and/or perivascular cells, appeared around the perivascular space at 6 h after traumatic SCI (Satake et al., 2000a). NO is known to cause the inflammation and the production of PGE_2 (Iyengar et al., 1987; Ialenti et al., 1992; Wong et al., 1996). In the present study, we observed that macrophages and endothelial cells co-existed along the pia matter and in blood vessels of the spinal cord 6 h after injury (Fig. 4). There are some reports on regulation of COX-2 activity and induction by NO using iNOS deficient mice (Guhring et al., 2000; Nogawa et al., 1998). Therefore, NO released by macrophage via iNOS seems to sustain high expression level of *COX-2* gene at least until 3 days after traumatic SCI since iNOS-positive cells were observed around the damaged area 2 days after the injury (Satake et al., 2000a). Further studies on the relationship of the mutual control between iNOS and COX-2 are required for development of better clinical treatments for patients who have suffered traumatic SCI.

5. Conclusion

COX-2 mRNA is induced within 30 min and COX-2 protein is increased in endothelial cells of blood vessels at 6 h following contusion injury of the spinal cord. *COX-2* gene induction after traumatic SCI seems not to require any new protein synthesis, and COX-2 protein accumulated in endothelial cells may be a component of the successive inflammatory processes in the damaged area.

References

Allen, A.R., 1914. Remarks on the histopathological changes in the spinal cord due to impact an experimental study. J. Nerv. Ment. Dis. 31, 141–147.

Breder, C.D., Saper, C.B., 1996. Expression of inducible cyclooxygenase mRNA in the mouse brain after systemic administration of bacterial lipopolysaccharide. Brain Res. 713, 64–69.

Chao, C.C., Lokensgard, J.R., Sheng, W.S., Hu, S., Peterson, P.K., 1997. IL-1-induced iNOS expression in human astrocytes via NF-κB. Neuroreport 8, 3163–3166.

DeWitt, D.L., 1991. Prostaglandin endoperoxide synthase: regulation of enzyme expression. Biochim. Biophys. Acta 1083, 121–134.

DeWitt, D.L., Smith, W.L., 1998. Primary structure of prostaglandin G/H synthase from sheep vesicular gland determined from the complementary DNA sequence. Proc. Natl. Acad. Sci. U.S.A. 85, 1412–1416.

Faden, A., 1993. Experimental neurobiology of central nervous system trauma. Crit. Rev. Neurobiol. 7, 175–186.

Fan, Z., Isobe, K., Kiuchi, K., Nakashima, I., 1995. Enhancement of nitric oxide production from activated macrophages by a purified form of ginsenoside (Rg1). Am. J. Chin. 23, 279–287.

Feng, L., Sun, W., Xia, Y., Tang, W., Chanmugam, P., Soyoola, E., Wilson, C.B., Hwang, D., 1993. Cloning two isoforms of rat cyclooxygenase: differential regulation of their expression. Arch. Biochem. Biophys. 307, 361–368.

Garavito, R.M., Malkowski, M.G., DeWitt, D.L., 2002. The structures of prostaglandin endoperoxide H synthases-1 and -2. Prostaglandins Other Lipid Mediat. 68–69, 129–152.

Guhring, H., Gorig, M., Mehmet, A., Coste, O., Zeilhofer, H.U., Pahl, A., Rehse, K., Brune, K., 2000. Suppressed injury-induced rise in spinal prostaglandin E2 production and reduced early thermal hyperalgesia in iNOS-deficient mice. J. Neurosci. 20, 6714–6720.

Ialenti, A., Ianaro, A., Moncada, S., Rosa, D.M., 1992. Modulation of acute inflammation by endogenous nitric oxide. Eur. J. Pharmacol. 211, 177–182.

Ichitani, Y., Shi, T., Haeggstrom, J.Z., Samuelsson, B., Hokfelt, T., 1997. Increased levels of cyclooxygenase-2 mRNA in the rat spinal cord after

peripheral inflammation: an in situ hybridization study. Neuroreport 8, 2949–2952.

Inoue, A., Ikoma, K., Morioka, N., Kumagai, K., Hashimoto, T., Hide, I., Nakata, Y., 1999. Interleukin-1 beta induces substance P release from primary afferent neurons through the cyclooxygenase-2 system. J. Neurochem. 73, 2206–2213.

Iyengar, R., Stuehr, D.J., Marletta, M.A., 1987. Macrophage synthesis of nitrite, nitrate, and N-nitrosamines: precursors and role of the respiratory burst. Proc. Natl. Acad. Sci. U.S.A. 84, 6369–6373.

Jobin, C., Morteau, O., Han, D.S., Sartor, R.B., 1998. Specific NF-κB blockade selectively inhibits tumour necrosis factor-α-induced COX-2 but not constitutive COX-1 gene expression in HT-29 cells. Immunology 95, 537–543.

Kujubu, D.A., Fletcher, B.S., Varnum, B.C., Lim, R.W., Herschman, H.R., 1991. TIS10, a phorbol ester tumor promoter-inducible mRNA from Swiss 3T3 cells, encodes a novel prostaglandin synthase/cyclooxygenase homologue. J. Biol. Chem. 266, 12866–12872.

Kujubu, D.A., Herschman, H.R., 1992. Dexamethasone inhibits mitogen induction of the TIS 10 prostaglandin synthase/cyclooxygenase gene. J. Biol. Chem. 267, 7991–7994.

Madrigal, J.L., Moro, M.A., Lizasoain, I., Lorenzo, P., Castrillo, A., Bosca, L., Leza, J.C., 2001. Inducible nitric oxide synthase expression in brain cortex after acute restraint stress is regulated by nuclear factor κB-mediated mechanisms. J. Neurochem. 76, 532–538.

Nakayama, M., Uchimura, K., Zhu, R.L., Nagayama, T., Rose, M.E., Stetler, R.A., Isakson, P.C., Chen, J., Graham, S.H., 1998. Cyclooxygenase-2 inhibition prevents delayed death of CA hippocampal neurons following global ischemia. Proc. Natl. Acad. Sci. U.S.A. 95, 10954–10959.

Nishiya, T., Uehara, T., Kaneko, M., Nomura, Y., 2000. Involvement of nuclear factor-κB (NF-κB) signaling in the expression of inducible nitric oxide synthase (iNOS) gene in rat C6 glioma cells. Biochem. Biophys. Res. Commun. 275, 268–273.

Nogawa, S., Forster, C., Zhang, F., Nagayama, M., Ross, M.E., Iadecola, C., 1998. Interaction between inducible nitric oxide synthase and cyclooxygenase-2 after cerebral ischemia. Proc. Natl. Acad. Sci. U.S.A. 95, 10966–10971.

O'Banion, M.K., Winn, V.D., Young, D.A., 1992. cDNA cloning and functional activity of a glucocorticoid-regulated inflammatory cyclooxygenase. Proc. Natl. Acad. Sci. U.S.A. 89, 4888–4892.

Otto, J.C., DeWitt, D.L., Smith, W.L., 1993. *N*-glycosylation of prostaglandin endoperoxide synthase-1 and -2 and their orientations in the endoplasmic reticulum. J. Biol. Chem. 268, 18234–18242.

Poligone, B., Baldwin, A.S., 2001. Positive and negative regulation of NF-κB by COX-2: roles of different prostaglandins. J. Biol. Chem. 276, 38658–38664.

Resnick, D.K., Graham, S.H., Dixon, C.E., Marion, D.W., 1998. Role of cyclooxygenase-2 in acute spinal cord injury. J. Neurotrauma. 15, 1005–1013.

Satake, K., Matsuyama, Y., Kamiya, M., Kawakami, H., Iwata, H., Adachi, K., Kiuchi, K., 2000a. Nitric oxide via macrophage iNOS induces apoptosis following traumatic spinal cord injury. Brain Res. Mol. Brain Res. 85, 114–122.

Satake, K., Matsuyama, Y., Kamiya, M., Kawakami, H., Iwata, H., Adachi, K., Kiuchi, K., 2000b. Up-regulation of glial cell line-derived neurotrophic factor (GDNF) following traumatic spinal cord injury. Neuroreport 11, 3877–3881.

Serou, M.J., DeCoster, M.A., Bazan, N.G., 1999. Interleukin-1 beta activates expression of cyclooxygenase-2 and inducible nitric oxide synthase in primary hippocampal neuronal culture: platelet-activating factor as a preferential mediator of cyclooxygenase-2 expression. J. Neurosci. Res. 58, 593–598.

Sirois, J., Levy, L.O., Simmons, D.L., 1993. Characterization and hormonal regulation of the promoter of the rat prostaglandin endoperoxide synthase 2 gene in granulosa cells. Identification of functional and protein-binding regions. J. Biol. Chem. 268, 12199–12206.

Smith, W.L., Garavito, R.M., DeWitt, D.L., 1996. Prostaglandin endoperoxide H synthases cyclooxygenases-1 and -2. J. Biol. Chem. 271, 33157–33160.

Tanaka, M., Ito, S., Kiuchi, K., 2000. Novel alternative promoters of mouse glial cell line-derived neurotrophic factor gene. Biochim. Biophys. Acta 1494, 63–74.

Tator, C.H., 1995. Update on the pathophysioloy and pathology of acute spinal cord injury. Brain Pathol. 5, 407–413.

Tator, C.H., Fehlings, M.G., 1991. Review of the secondary injury theory of acute spinal cord trauma with emphasis on vascular mechanisms. J. Neurosurg. 75, 15–26.

Tonai, T., Taketani, Y., Ueda, N., Nishisho, T., Ohmoto, Y., Sakata, Y., Muraguchi, M., Wada, K., Yamamoto, S., 1999. Possible involvement of interleukin-1 in cyclooxygenase-2 induction after spinal cord injury in rats. J. Neurochem. 72, 302–309.

Wong, M.L., Rettori, V., AL-Shekhlee, A., Bongiorno, P.B., Canteros, G., McCann, S.M., Gold, P.W., Licinio, J., 1996. Inducible nitric oxide synthase gene expression in the brain during systemic inflammation. Nat. Med. 2, 581–584.

Yamagata, K., Andreasson, K.I., Kaufmann, W.E., Barnes, C.A., Worley, P.F., 1993. Expression of a mitogen-inducible cyclooxygenase in brain neurons: regulation by synaptic activity and glucocorticoids. Neuron 11, 371–386.

Yamamoto, K., Arakawa, T., Ueda, N., Yamamoto, S., 1995. Transcriptional roles of nuclear factor kappa B and nuclear factor-interleukin-6 in the tumor necrosis factor alpha-dependent induction of cyclooxygenase-2 in MC3T3-E1 cells. J. Biol. Chem. 270, 31315–31320.

Available online at www.sciencedirect.com
SCIENCE DIRECT
Virus Research 108 (2005) 23–28
Virus Research
www.elsevier.com/locate/virusres

A lentiviral expression system demonstrates that L* protein of Theiler's murine encephalomyelitis virus (TMEV) is essential for virus growth in a murine macrophage-like cell line

Toshiki Himeda[a], Yoshiro Ohara[a,*], Kunihiko Asakura[a], Yasuhide Kontani[a], Manabu Murakami[b], Hiromi Suzuki[c], Makoto Sawada[c]

[a] *Department of Microbiology, Kanazawa Medical University, 1-1 Uchinada, Ishikawa 920 0293, Japan*
[b] *Division of Basic Science, Medical Research Institute, Kanazawa Medical University, 1-1 Uchinada, Ishikawa 920 0293, Japan*
[c] *Institute for Comprehensive Medical Science, Fujita Health University, Aichi 470 1192, Japan*

Received 14 April 2004; received in revised form 14 July 2004; accepted 19 July 2004
Available online 17 September 2004

Abstract

The DA subgroup strains of Theiler's murine encephalomyelitis virus (TMEV) synthesize L* protein, which is translated out of frame with the polyprotein from an alternative AUG, 13 nucleotides downstream from the authentic polyprotein AUG. By a 'loss of function' experiment using a mutant virus, DAL*-1, in which the L* AUG is mutated to an ACG, L* protein is shown to play an important role in virus persistence, TMEV-induced demyelination, and virus growth in macrophages. In the present study, we established an L* protein-expressed macrophage-like cell line and confirmed the importance of L* protein in virus growth in this cell line.

Keywords: Theiler's murine encephalomyelitis virus; L* protein; Lentiviral vector; Virus growth; Macrophages

Theiler's murine encephalomyelitis virus (TMEV) belongs to the genus *Cardiovirus* of the family *Picornaviridae* and is divided into two subgroups (Ohara and Roos, 1987; Lipton and Jelachich, 1997; Obuchi and Ohara, 1998; Roos, 2002). DA (or TO) subgroup strains induce a non-fatal polioencephalomyelitis in weanling mice followed by virus persistence and chronic demyelination in the spinal cords. This late demyelinating disease serves as an experimental model of the human demyelinating disease, multiple sclerosis. In contrast, GDVII subgroup strains cause acute fatal polioencephalomyelitis without demyelination. The precise mechanisms of virus persistence and demyelination caused by DA subgroup strains are still unknown. A 17 kDa protein, called L*, is translated out of frame with the polyprotein from an alternative AUG, 13 nucleotides downstream from the authentic polyprotein AUG (Kong and Roos, 1991; Obuchi and Ohara, 1998; Roos, 2002). L* protein is only synthesized in the DA subgroup strains since the L* AUG is present in DA subgroup strains, but not in GDVII subgroup strains (Michiels et al., 1995; Obuchi and Ohara, 1998; Roos, 2002). Therefore, L* protein is thought to be a key protein regulating DA biological activities. A 'loss-of-function' experiment using a mutant virus, DAL*-1, in which the L* AUG initiation codon is mutated to an ACG, demonstrated that L* protein plays an important role in DA persistence and demyelination (Chen et al., 1995; Ghadge et al., 1998). However, that finding is still controversial since the absence of the L* AUG initiation codon in a different DA infectious clone had only a weak influence on the persistence of DA strain (van Eyll and Michiels, 2000, 2002).

We previously reported that DA strain grows in J774-1 cells, an *H-2*^{d} macrophage-like cell line derived from a tumor of a BALB/c mouse (Ralph et al., 1975), while the GDVII

* Corresponding author. Tel.: +81 76 218 8096; fax: +81 76 286 3961.
E-mail address: ohara@kanazawa-med.ac.jp (Y. Ohara).

0168-1702/$ – see front matter © 2004 Elsevier B.V. All rights reserved.
doi:10.1016/j.virusres.2004.07.009

strain does not (Obuchi et al., 1997). This phenomenon is of great interest since a major site for TMEV persistence is thought to be macrophages (Lipton and Jelachich, 1997; Obuchi and Ohara, 1998; Roos, 2002). The important role of L* protein in this in vitro phenomenon can be demonstrated by using DAL*-1 virus. DAL*-1 virus does not grow in murine monocyte/macrophage lineage cell lines, but it does grow in other cell lines, including neural cells (Obuchi et al., 1999). A recombinant virus, DANCL*/GD, which has the DA 5′ noncoding and L* protein coding regions replacing the corresponding regions of GDVII and therefore synthesizes L* protein, had a rescue of growth activity in J774-1 cells, suggesting that L* protein plays an important role in virus growth in macrophages (Obuchi et al., 2000).

A challenge in research related to L* protein is that its sequence overlaps with that of the polyprotein, making it impossible to introduce the DA L* coding sequence into the parental GDVII strain without changing the polyprotein sequence. The generation of macrophage cells that constitutively express L* protein would allow a confirmation of the role of this protein in virus growth with a 'gain of function' experiment. This system would also allow the synthesis of L* protein in the cytoplasm, as has been described (Obuchi et al., 2001), without being incorporated into virions. Therefore, the goal of the present study was to establish a macrophage cell line that constitutively expresses L* protein.

We used a lentiviral expression system in order to achieve a stable and efficient gene transfer of L* protein. The vector was constructed by using the transfer vector plasmid pCSII-EF-MCS-IRES-hrGFP, constructed by Dr. Hiroyuki Miyoshi and Dr. Tomoyuki Yamaguchi, Laboratory of Genetics, The Salk Institute for Biological Studies. The plasmid has sequences of a human elongation factor (EF) 1 α subunit gene promoter, a multiple cloning site (MCS), an internal ribosome entry site (IRES), and the coding region of a 'humanized, red-shifted' green fluorescent protein (hrGFP) in tandem. L* coding sequence was inserted into MCS, resulting in the production of L* protein independently from hrGFP and not as a fusion protein. The expression of both proteins is regulated by one promoter. Another construct, in which the 3xFLAG epitope sequence is tagged to the N-terminus of L* protein, was generated as an additional control since the 5′ one third of the L* protein coding region is important for its function (Obuchi et al., 2001). In order to generate vesicular stomatitis virus (VSV) G protein-pseudotyped lentiviral vector particles, the transfer vector plasmid pCSII-EF-(cDNA of L* or 3xFLAGL* protein)-IRES-hrGFP with the packaging plasmid pMDLg/pRRE, pRSV-Rev, and the VSV-G protein envelope plasmid pMD.G (Naldini et al., 1996) were tansfected into subconfluent 293T cells, a human embryonic kidney epithelial cell line expressing the simian virus 40 large T antigen, using a high-efficiency calcium-phosphate-mediated transfection method (Miyoshi et al., 1997; Miyoshi et al., 1998; Sambrook and Russell, 2001). High-titer virus stocks were prepared by centrifugation (43,600 × *g*, 3 h, 21 °C). The infectious titers were determined by counting the number of GFP-positive cells by fluorescence-activated cell sorting (FACS) analysis (FACSCalibur: BD Biosciences, San Jose, CA). J774-1 cells (2×10^5) were infected and transduced at a multiplicity of infection (M.O.I.) of 5. After the infection, the third subculture of L*-transduced and 3xFLAGL*-transduced J774-1 cells were seeded at a density of 0.5 cells per well onto 360 wells and 1200 wells of HLA plates (Greiner bio-one, Tokyo, Japan), respectively.

Cell propagation was observed in 27 wells of L*-transduced cells and 105 wells of 3xFLAGL*-transduced cells. During the first several passages, the cells in approximately 50% of wells were GFP-positive and propagated more slowly than the original J774-1 cells. Some showed a different morphology, such as enlargement (20–30 μm, about 1.5-fold larger in diameter) and an amoebic shape. We selected four L*-expressed (L*/J774) and eight 3xFLAGL*-expressed (3xFLAGL*/J774) clones by FACS analysis using expression of GFP. The cells formed clusters easily when replated in new culture dishes. These properties reverted to those of the original J774-1 cells after seven passages. When both cells were seeded in a 35 mm plastic culture dish at the density of 1×10^5 cells/ml, the cultures reached to the density of 1×10^6 cells/ml within about four days, with a doubling time of 24–30 h. Seven empty vector-transduced clones (control/J774) were also obtained from the empty vector-transduced J774-1 cells and served as a control. The properties of these cells were not different from those of the original J774-1 cells. Fig. 1 shows the histograms of L*/J774/6, 3xFLAGL*/J774/33 and control/J774/6 clones, which gave the highest GFP expression.

The expression of L* and 3xFLAGL* proteins was further confirmed by Western blotting using polyclonal rabbit anti-L* antibody (Ab) (Obuchi et al., 2000, 2001) or monoclonal mouse anti-FLAG M2 Ab (Sigma, St. Louis, MO). Enhanced chemiluminescence reagents, ECL plus (Amersham Biosciences, Buckinghamshire, UK), detected biotinylated secondary Ab and horseradish peroxidase-conjugated streptavidin (Fig. 2). The expression of L* or 3xFLAGL* protein was stable after forty passages of culture.

We examined and compared the growth kinetics of DAL*-1 virus in those cells. The culture supernatants and cell lysates of 1.5×10^6 cells infected with DAL*-1 virus at an M.O.I. of 10 PFU per cell were harvested at 0, 3, 6, 12, 24, and 48 h post-infection (p.i.), and the infectivity was assayed by a standard plaque assay on BHK-21 cells. In L*/J774/6 cells, the titers of cell-free and cell-associated DAL*-1 virus reached a peak at 12 h p.i. (6.3×10^5 and 3.8×10^5 PFU/ml, respectively) and then gradually decreased (Fig. 3B). On the other hand, the titers gradually decreased in control/J774/6 cells (Fig. 3A). The data indicated that L* protein is essential for DA growth in J774-1 cells. The titers of DAL*-1 virus also gradually decreased in 3xFLAGL*/J774/33 cells (Fig. 3C), suggesting that the N-terminus is important for the function of L* protein, as previously reported (Obuchi et al., 2001). In addition, even though the 3xFLAG epitope is a small peptide (2.7 kDa), it may have changed the higher-order structure of

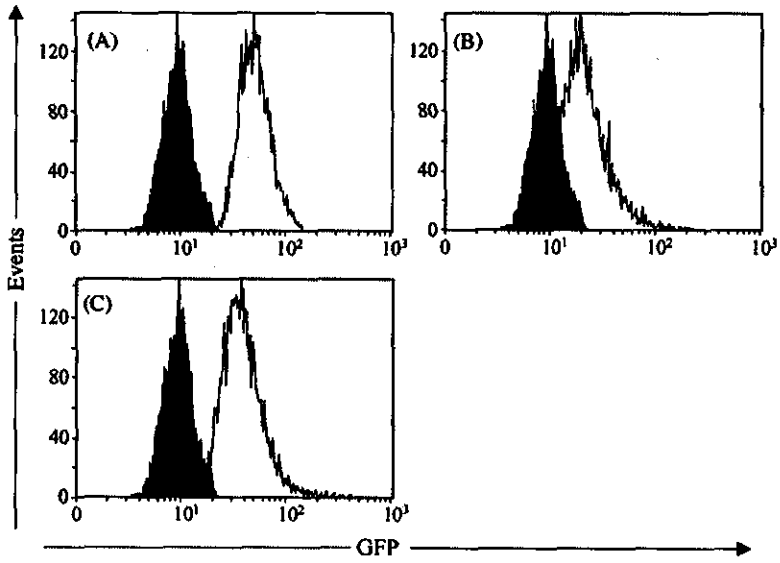

Fig. 1. Flow cytometric analysis of green fluorescent protein (GFP) fluorescence. J774-1 cells were infected and transduced with lentiviral vector containing the L* or 3xFLAGL* protein sequence. The transduced cells were cloned by a limiting dilution. Figure shows the histograms of GFP fluorescence in the representative clone of the vector-transduced J774-1 cells (open area). The original J774-1 cells served as a control (closed area). (A) Control/J774/6, which was transduced by an empty vector as described in the text; (B) L*/J774/6, which was transduced by the vector containing the L* sequence; (C) 3xFLAGL*/J774/33, which was transduced by the vector containing the 3xFLAGL* sequence.

L* protein since L* protein is relatively small (17 kDa). Also, the predicted hydrophilicity of 3xFLAG epitope may have interfered with the strong hydrophobicity of L* protein (Ohara et al., 1988; Obuchi et al., 2001), and thereby disturbed the function of L* protein.

To further investigate which step of virion formation is affected by L* protein, viral RNA synthesis of DAL*-1 virus following the infection of those cells was analyzed by RNase protection assay (RPA) (Fig. 4A). RPA was performed with the BD RiboQuant™ Non-Radioactive RPA system (BD Biosciences, San Jose, CA), according to the manufacturer's instructions. Briefly, pDAFL3, a full-length infectious DA cDNA clone (Roos et al., 1989), was cleaved at the *Hinc*II site (nt 7783) in the viral genome in order to prepare an antisense probe. The linearized plasmid was transcribed by an in vitro transcription system with T3 RNA polymerase in the presence of biotin-16-UTP (Roche Diagnostics GmbH, Mannheim, Germany). The biotin-labeled RNA probe con-

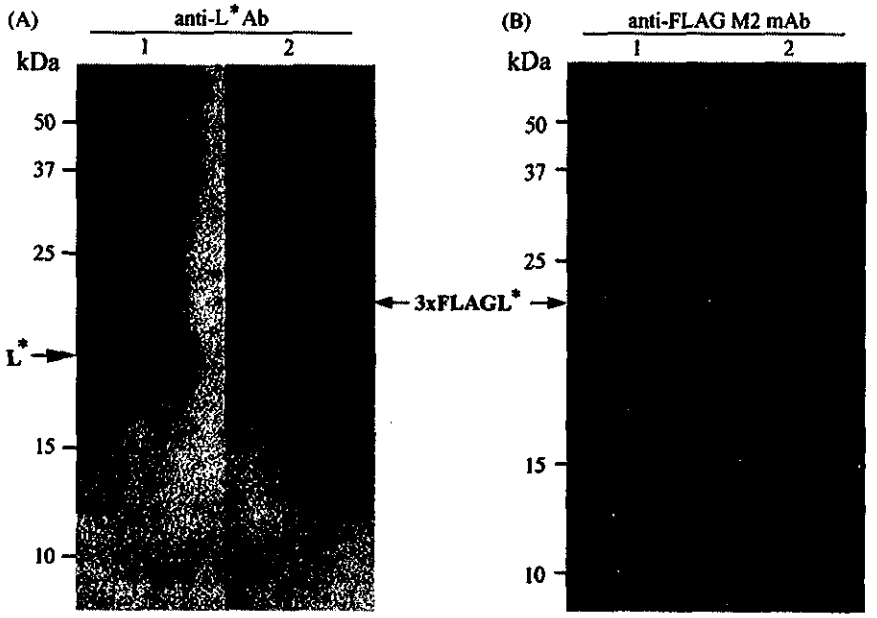

Fig. 2. Protein expression of the transgenes (L* and 3xFLAGL* sequences) in L*/J774/6 and 3xFLAGL*/J774/33 cells. The expression of L* gene in L*/J774/6 cells or 3xFLAGL* gene in 3xFLAGL*/J774/33 cells was analyzed by Western blotting as described in the text. L* (lane 1) and 3xFLAGL* (lane 2) proteins were detected with anti-L* antibody (A) and anti-FLAG M2 monoclonal antibody (B), respectively.

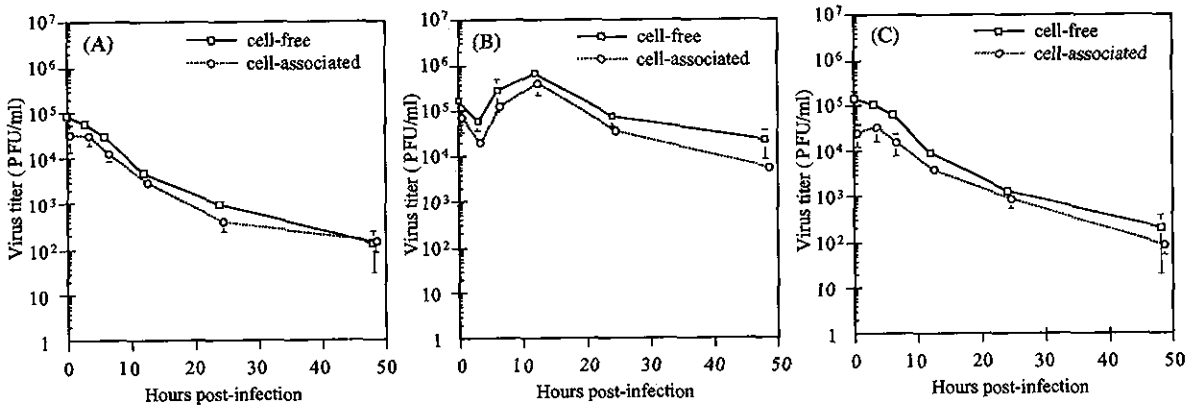

Fig. 3. Growth kinetics of DAL*-1 virus in control/J774/6 (A), L*/J774/6 (B), and 3xFLAGL*/J774/33 (C) cells. The culture supernatants (solid lines, open squares) and cell lysates (broken lines, open circles) of cells infected at a multiplicity of infection (M.O.I.) of 10 were harvested at indicated time points and subjected to titer determination by a standard plaque assay on BHK-21 cells. Data are expressed as the mean ± standard deviation (S.D.) in three independent experiments.

tained 310 nt of sequence complementary to the 3' region of the viral genome and 52 nt of vector sequence (Ohara et al., 1988; Roos et al., 1989). At 0, 3, 6, and 9 h p.i., total RNA was extracted and purified from 9.3×10^4 virus-infected cells by using RNeasy Mini Kit (QIAGEN, Tokyo, Japan). The RNA and 10 ng of biotin-labeled RNA probe were hybridized, and then treated with RNase A and RNase T1. The protected RNA probes were separated by electrophoresis on 5% polyacrylamide gels containing 8 M urea, and transferred to positively-charged nylon membranes by electroblotting. The signals were detected by chemiluminescent detection system. As shown in Fig. 4A, the amount of viral RNA of DAL*-1 virus clearly increased and reached a peak 6 h p.i. in all the cells examined.

Viral protein synthesis was also examined in those cells. At 3, 6, and 9 h p.i., 1×10^6 cells infected with DAL*-1 virus were scraped and dissolved in sample buffer (0.01 M Tris-Cl [pH 6.8], 1 mM EDTA, 2.5% SDS, 5% 2-mercaptoethanol, 10% glycerol, 0.005% bromophenol blue). The cell lysates were analyzed by Western blotting with DA-neutralizing monoclonal antibody, DA mAb 2, which reacts to VP1 capsid protein of DA strain (kindly provided from Dr. Raymond P. Roos, University of Chicago, IL) (Fig. 4B). The amount of VP1 capsid protein of DAL*-1 virus increased rapidly from

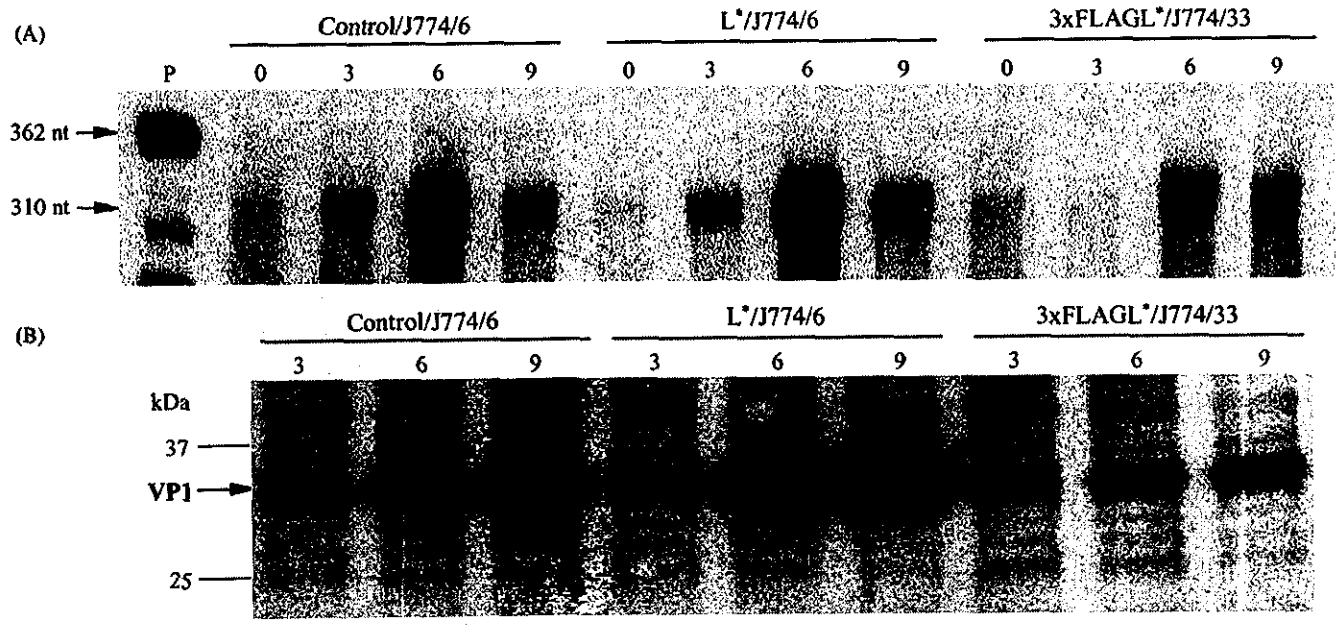

Fig. 4. (A) Viral RNA synthesis of DAL*-1 virus in control/J774/6, L*/J774/6, and 3xFLAGL*/J774/33 cells. Total RNA extracted from the virus infected-cells (9.3×10^4 cells) was subjected to RNase protection assay as described in the text. The numbers at the top of panel indicate hours post-infection (p.i.). Lane P is the starting probe. (B) Synthesis of viral protein in control/J774/6, L*/J774/6, and 3xFLAGL*/J774/33 cells. The cells were infected with DAL*-1 virus at an M.O.I. of 10. After the infection, the cell lysates were analyzed by Western blotting with DA mAb 2 as described in the text. The numbers at the top of panel indicate hours p.i.

3 h p.i., reaching a plateau at 6 to 9 h p.i. in L*/J774/6 cells. The same tendency was observed in both control/J774/6 and 3xFLAGL*/J774/33 cells.

The data obtained in the L*-expressed system have confirmed that L* protein is essential for virus growth in J774-1 cells. In fact, GDVII strain, which does not grow in J774-1 cells (Obuchi et al., 1997), also had a rescue of the growth activity in L*/J774/6 cells (data not shown). As described elsewhere (Obuchi et al., 1997), DA strain infects and actively replicates in J774-1 cells, with only a minimal damage on these cells. This property is clearly important to set the stage for a persistent infection of DA strain in macrophages in vivo. Therefore, DA strain may be able to maintain its genome in macrophages in the presence of L* protein, leading to virus persistence and consequently to demyelination.

As shown in Fig. 4A and B, L* protein had no effects on viral RNA replication and viral protein translation. These results differ from our previous reports (Takata et al., 1998; Obuchi et al., 1999, 2000) that suggested that L* protein probably interferes with viral RNA replication, however, only two time-points (3 and 9 h p.i.) were examined in these previous studies. No effects of L* protein on virus attachment were found in a previous report (Obuchi et al., 1999). As shown in Fig. 3, the titers of cell-associated virus almost paralleled those of cell-free virus in all cells, strongly suggesting that the release of virions are not influenced by the presence or the absence of L* protein. Therefore, L* protein may have some effect(s) on the step of virion assembly. The effect of L* protein is presumably in *trans*.

The formation of viral particles of picornaviruses is reported to be coupled to RNA replication, both events occurring on the surface of virus-induced membranous vesicles found in the cytoplasm of infected cells (Blondel et al., 1998). The poliovirus-induced vesicles are formed closely related on the surface of intracellular membranes, such as the endoplasmic reticulum (ER) (Suhy et al., 2000). Proteins of the poliovirus replication complex, especially 2BC and 3A, accumulate in patches on the ER. Double membrane vesicles derive from the ER (Suhy et al., 2000). Microtubules are known to be closely associated with the ER (Lodish et al., 1995). It may be that the association of L* protein with microtubules is important in TMEV assembly in J774-1 cells or other macrophage cell lines. Of interest, the importance of L* protein to DA growth is not observed in other types of cells (Obuchi et al., 1999). Some unknown host cell factor(s) may have a key interaction with L* protein that is important for virus growth. This may foster DA persistence in a cell key to carrying out DA-induced demyelination. Two-hybrid system may identify this factor(s), and the study is under progress. The restricted growth and persistence of TMEV in macrophages may be critical to the white matter disease. Therefore, the identification of this factor(s) interacting with L* protein may clarify the mechanism(s) of TMEV-induced demyelinating disease.

Acknowledgements

This work was supported by a Grant-in-Aid for Scientific Research from the Ministry of Education, Science, Sports and Culture; and a Grant for Project Research from High-Technology Center of Kanazawa Medical University (H2002-7) and a Grant for Promoted Research from Kanazawa Medical University (S2003-5).

References

Blondel, B., Duncan, G., Couderc, T., Delpeyroux, F., Pavio, N., Colbere-Garapin, F., 1998. Molecular aspects of poliovirus biology with a special focus on the interactions with nerve cells. J. NeuroVirol. 4, 1–26.

Chen, H.-H., Kong, W.-P., Zhang, L., Ward, P.L., Roos, R.P., 1995. A picornaviral protein synthesized out of frame with the polyprotein plays a key role in a virus-induced immune-mediated demyelinating disease. Nat. Med. 1, 927–931.

Ghadge, G.D., Ma, L., Sato, S., Kim, J., Roos, R.P., 1998. A protein critical for a Theiler's virus-induced immune system-mediated demyelinating disease has a cell type-specific antiapoptotic effect and a key role in virus persistence. J. Virol. 72, 8605–8612.

Kong, W.-P., Roos, R.P., 1991. Alternative translation initiation site in the DA strain of Theiler's murine encephalomyelitis virus. J. Virol. 65, 3395–3399.

Lipton, H.L., Jelachich, M.L., 1997. Molecular pathogenesis of Theiler's murine encephalomyelitis virus-induced demyelinating disease in mice. Intervirology 40, 143–152.

Lodish, H., Baltimore, D., Berk, A., Zipursky, S.L., Matsudaira, P., Darnell, J., 1995. Microtubules and intermediate filaments. In: Lodish, H., Baltimore, D., Berk, A., Zipursky, S.L., Matsudaira, P., Darnell, J. (Eds.), Molocular cell biology, third ed. Scientific American books, New York, pp. 1072–1075.

Michiels, T., Jarousse, N., Brahic, M., 1995. Analysis of the leader and capsid coding regions of persistent and neurovirulent strains of Theiler's virus. Virology 214, 550–558.

Miyoshi, H., Takahashi, M., Gage, F.H., Verma, I.M., 1997. Stable and efficient gene transfer into the retina using an HIV-based lentiviral vector. Proc. Natl. Acad. Sci. U.S.A. 94, 10319–10323.

Miyoshi, H., Blömer, U., Takahashi, M., Gage, F.H., Verma, I.M., 1998. Development of a self-inactivating lentivirus vector. J. Virol. 72, 8150–8157.

Naldini, L., Blömer, U., Gallay, P., Ory, D., Mulligan, R., Gage, F.H., Verma, I.M., Trono, D., 1996. In vivo gene delivery and stable transduction of nondividing cells by a lentiviral vector. Science 272, 263–267.

Obuchi, M., Ohara, Y., Takegami, T., Murayama, T., Takada, H., Iizuka, H., 1997. Theiler's murine encephalomyelitis virus subgroup strain-specific infection in a murine macrophage-like cell line. J. Virol. 71, 729–733.

Obuchi, M., Ohara, Y., 1998. Theiler's murine encephalomyelitis virus and mechanisms of its persistence. Neuropathology 18, 13–18.

Obuchi, M., Yamamoto, J., Uddin, M.N., Odagiri, T., Iizuka, H., Ohara, Y., 1999. Theiler's murine encephalomyelitis virus (TMEV) subgroup strain-specific infection in neural and non-neural cell lines. Microbiol. Immunol. 43, 885–892.

Obuchi, M., Yamamoto, J., Odagiri, T., Uddin, M.N., Iizuka, H., Ohara, Y., 2000. L* protein of Theiler's murine encephalomyelitis virus is required for virus growth in a murine macrophage-like cell line. J. Virol. 74, 4898–4901.

Obuchi, M., Odagiri, T., Asakura, K., Ohara, Y., 2001. Association of L* protein of Theiler's murine encephalomyelitis virus with microtubules in infected cells. Virology 289, 95–102.

Ohara, Y., Roos, R.P., 1987. The antibody response in Theiler's virus infection: new perspectives on multiple sclerosis. Prog. Med. Virol. 34, 156–179.

Ohara, Y., Stein, S., Fu, J., Stillman, L., Klaman, L., Roos, R.P., 1988. Molecular cloning and sequence determination of DA strain of Theiler's murine encephalomyelitis viruses. Virology 164, 245–255.

Ralph, P., Prichard, J., Cohn, M., 1975. Reticulum cell sarcoma: An effector cell in antibody-dependent cell-mediated immunity. J. Immunol. 114, 898–905.

Roos, R.P., Stein, S., Ohara, Y., Fu, J., Semler, B.L., 1989. Infectious cDNA clones of the DA strain of Theiler's murine encephalomyelitis virus. J. Virol. 63, 5492–5496.

Roos, R.P., 2002. Pathogenesis of Theiler's murine encephalomyelitis virus-induced disease. In: Semler, B.L., Wimmer, E. (Eds.), Molecular Biology of Picornaviruses. ASM Press, Washington, DC, pp. 427–435.

Sambrook, J., Russell, D.W., 2001. Alternative protocol: high-efficiency calcium-phosphate-mediated transfection of eukaryotic cells with plasmid DNAs, third ed. In: Sambrook, J., Russell, D.W. (Eds.), Molecular Cloning: A Laboratory Manual, vol. 3. Cold Spring Harbor Laboratory Press, Cold Spring Harbor, New York, pp. 16.19–16.20.

Suhy, D.A., Giddings Jr., T.H., Kirkegaard, K., 2000. Remodeling the endoplasmic reticulum by poliovirus infection and by individual viral proteins: an autophagy-like origin for virus-induced vesicles. J. Virol. 74, 8953–8965.

Takata, H., Obuchi, M., Yamamoto, J., Odagiri, T., Roos, R.P., Iizuka, H., Ohara, Y., 1998. L* protein of DA strain of Theiler's murine encephalomyelitis virus is important for virus growth in a murine macrophage-like cell line. J. Virol. 72, 4950–4955.

van Eyll, O., Michiels, T., 2000. Influence of the Theiler's virus L* protein on macrophage infection, viral persistence, and neurovirulence. J. Virol. 74, 9071–9077.

van Eyll, O., Michiels, T., 2002. Non-AUG-initiated internal translation of the L* protein of Theiler's virus and importance of this protein for viral persistence. J. Virol. 76, 10665–10673.